Covalent organic frameworks for environmental analysis

Hai-Long Qian [a, b, c, *], Yan Wang [c], Xiu-Ping Yan [a, b, c, **]

[a] State Key Laboratory of Food Science and Technology, Jiangnan University, Wuxi 214122, China
[b] Key Laboratory of Synthetic and Biological Colloids, Ministry of Education, School of Chemical and Material Engineering, Jiangnan University, Wuxi, 214122, China
[c] Institute of Analytical Food Safety, School of Food Science and Technology, Jiangnan University, Wuxi 214122, China

ARTICLE INFO

ABSTRACT

As typical representative of porous crystalline polymers, covalent organic frameworks (COFs) based on dynamic covalent chemistry and topological design are constructed with organic units via covalent bond. Their unique properties such as high stability, accessible functionality, ordered porosity, and pre-designable structure make COFs highly promising in environmental analysis. This review highlights the state-of-the-art design and modification of COFs in terms of functionality, stability and pore to meet the requirements of environmental analysis, as well as the mechanism and application of the COFs for the adsorption/removal, separation and sensing of various environmental contaminants. In addition, the challenge and future direction of COFs in environmental analysis are outlooked for the further research.

© 2022 Elsevier B.V. All rights reserved.

1. Introduction

Covalent organic frameworks (COFs) based on dynamic covalent chemistry (DCC) and topological design are constructed with organic units via covalent bond [1–4]. The reversible covalent bond of DCC dominated by thermodynamic reaction allows the self-healing feedback during the condensation of organic monomers. Thus, a thermodynamically stable ordered structure of COFs with crystallinity can be obtained by controlling synthetic conditions such as the reaction media, temperature and time [5–8]. Topological design will guide the connection of organic monomers and make sure the formation of the network for COFs in a predictive manner. The geometry and dimension of building monomers play crucial roles in topological design. The building monomers must own specific geometry with rigid structure to realize the predicted topology. The different knots and linkers of monomers give various topology of COFs [9–11]. Generally, the planar structure of monomers leads to two-dimensional (2D) COFs, while the tetrahedral structure of monomers forms three-dimensional (3D) COFs. The tunable covalent bond and topology can produce a large number of

COFs such as boronate-, imine-, hydrazone-, azine-, imide- and triazine-linked COFs with hexagonal, tetragonal, rhombic, kagome, trigonal, ctn, bor, dia, pts, and rra structures [9,10,12].

The unique properties make COFs highly promising for diverse applications [13–15]. The good chemical stability provided by co-valent bond allows the utilization of COFs in complex and harsh conditions [16]. The pre-designable and ordered crystalline struc-ture with uniform pore distribution endows COFs with rapid mass transfer for guest molecules [17]. The high surface area of COFs makes sure the sufficient active sites to interact with guest mole-cules. The tunable functionality brings COFs the specific in-teractions to improve the selectivity in light of targets [18,19]. The extended layer of 2D COFs with π-conjugation makes COFs excel-lent sensors for chemical sensing [2]. To date, COFs have attracted great attention in analytical chemistry, especially environmental analysis [13,20–23]. As the analysis of trace analytes in environ-ment samples always suffers from the serious interference from complex matrix and structural analogues, COFs are engineered in the functionality, stability and pore to meet the demands of envi-ronmental analysis. An overview on the engineering COFs as adsorbent, stationary phase and sensor for analysis of environment contaminants is lacked.

In this review, we focus on the forefront of advanced COFs in environmental analysis (Fig. 1). The summaries of the design and modification of COFs in functionality, stability and pore to meet the requirements of environmental analysis will inspire the synthesis of more advanced COFs for diverse applications. The discussed

---

* Corresponding author. State Key Laboratory of Food Science and Technology, Jiangnan University, Wuxi 214122, China.
** Corresponding author. State Key Laboratory of Food Science and Technology, Jiangnan University, Wuxi 214122, China.
E-mail addresses: hlqian@jiangnan.edu.cn (H.-L. Qian), xpyan@jiangnan.edu.cn (X.-P. Yan).
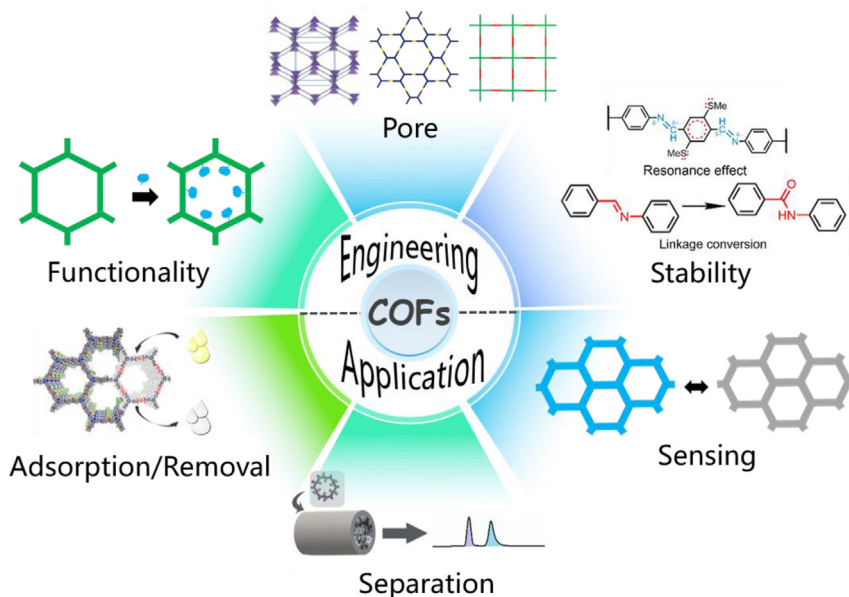
Fig. 1. Engineering the functionality, stability and pore of COFs for the application in environmental analysis.

mechanism and application of COFs in adsorption/removal, separation and sensing of various environmental contaminants can guide the future researches of COFs for environmental analysis. Furthermore, the perspective on the challenge and future direction for COFs in environmental analysis is also provided for the promotion of the development of COFs in environmental analysis.

2. Design and modification of COFs for environmental analysis

Up to date, various COFs have already been applied in environmental analysis (Fig. 2 and Table 1). In order to meet the requirements of environmental analysis, COFs were designed and modified in terms of functionality, stability and pore. Since the analytes in the environment are always trace amounts and seriously interfered from complex matrix and structural analogues, the introduction of functional groups into COFs through bottom-up [16,24—27] and post-modification [28—31] is essential to promote the selectivity of COFs for the environmental contaminants. For example, the anchor of chelating soft base groups made COFs promising as selective adsorbents/sensors for the removal/sensing of heavy metals [16,29,32]. The application of ionic units brought ionic covalent organic frameworks (iCOFs) excellent ionic exchange and electrostatic character for the extraction/removal of various radioactive pollutants [24,33—36]. The introduction of chiral centers made COFs suitable for chiral chromatography separation and sensing of enantiomer pollutants [37—40]. The combination of electrode with COFs endowed the sensing of harmful gas [31].

In addition to functionality, the stability is another important issue for application of COFs in environmental analysis due to the complex and harsh conditions of environmental samples. Imine-linked COFs first show great potential in adsorption/removal, separation and sensing owing to their high stability and crystallinity [27,41—43]. However, more stable COFs should be prepared for the utilization in harsh matrix such as strong acid and alkali. Thus, various approaches have been developed to enhance the stability of COFs. The introduction of intramolecular hydrogen bond in imine-linked COFs allowed the evident improvement of their stability [44]. The application of highly planar building blocks can also improve the stability, crystallinity and adsorption performance of

COFs by increasing the interlayer force [45]. Integrating resonance effect into 2D COFs can weaken the interlayer repulsive force and highly enhance the stability of 2D COFs [16]. Linkage conversion was another way to enhance the stability of COFs. The conversion of reversible imide-linked COFs to irreversible amide-linked COFs via building block exchange not only enhanced the stability of COFs, but also gave unique functionality [46].

Pore also shows great influence on the kinetics of environmental analytes on COFs. 2D COFs with ordered one-dimensional pore channels formed by covalent bond (intralayer) and weak interactions (interlayers) were widely used in rapid adsorption/removal, separation and sensing of environmental pollutants [43,47—49]. In contrast to 2D COFs, 3D COFs are linked with complete covalent bonds and possess richer pore structures (channels and cages), rendering them more benefits for interaction with the analytes [10]. Recently, a variety of 3D COFs started to show their potential as adsorbents, stationary phase and sensor in environmental analysis [32,50—55]. Heteroporous COFs also attracted wide attention in environmental analysis owing to the great potential in the reduction of diffusion barrier and simultaneous interactions with different sizes of molecules [49,56—58].

3. Applications in environmental analysis

3.1. Adsorption/removal

The ordered crystalline structure linked with covalent bond gives COFs high stability and accessibility of active sites to analytes. The tunable functionality further renders COFs diverse desired interactions with analytes. The phenylboronic acid and its derivative are well known for the selective and reversible interaction with *cis*-diol-containing compounds [73]. Hence, our group synthesized a phenylboronic acid functionalized COF (DhaTab-PBA) via the thiol-ene click reaction to adsorb/remove *cis*-diol catechol. The introduced boronic acid group evidently improved the selectivity of DhaTab-PBA for the adsorption of catechol in water with fast kinetics. The DhaTab-PBA gave 1.1—4.6 times higher adsorption capacity (133.3—151.5 mg g^{-1}) for catechol in real water samples than other adsorbents [28].
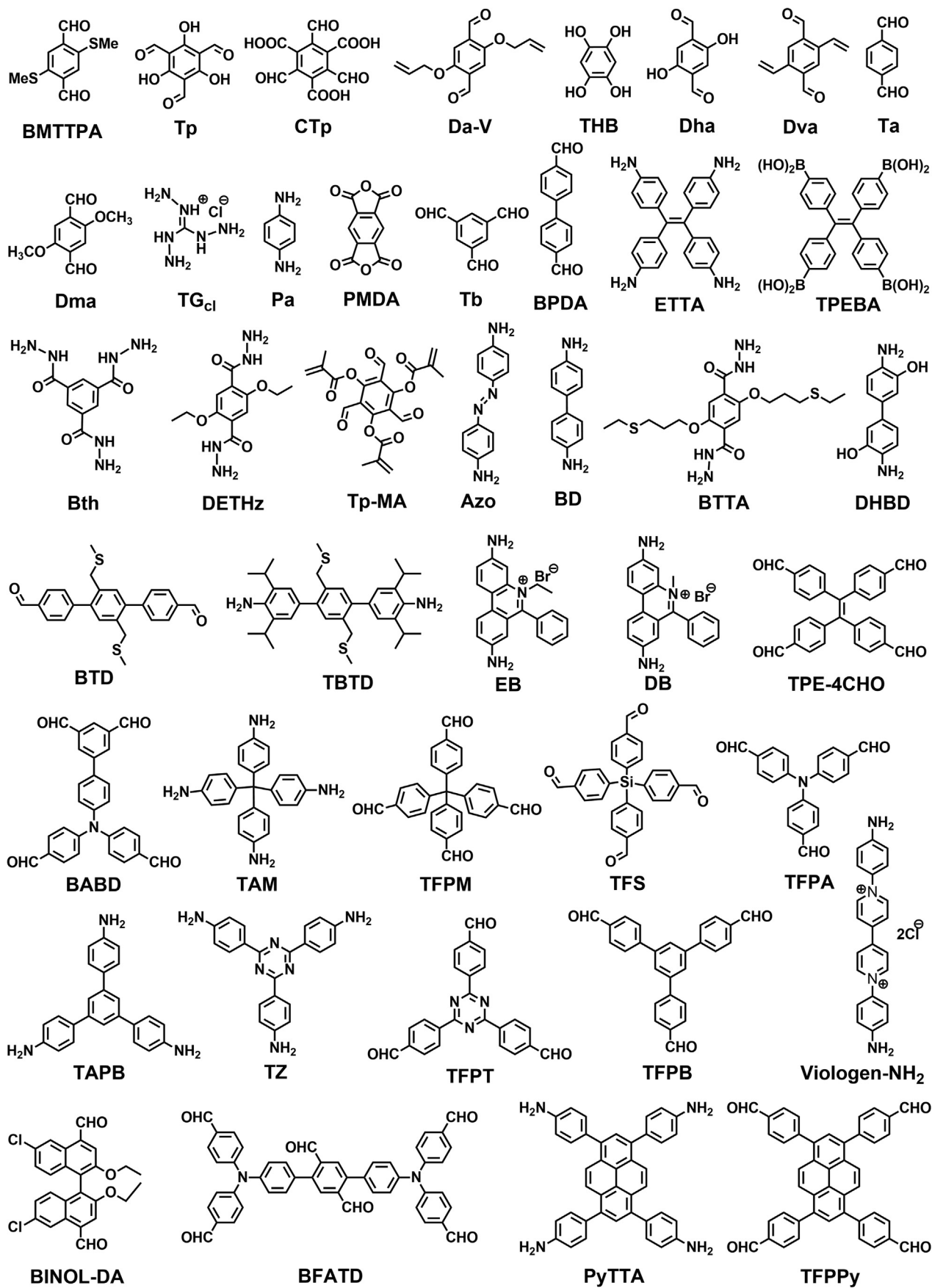
Fig. 2. Chemical structure of the building monomers for typical COFs in environmental analysis.

Table 1
Composition and application of typical COFs in environmental analysis.

COFs	Building monomer	Analyte	Applications	Refs
TAPB-BMTTPA-COF	1,3,5-Tris(4-aminophenyl)benzene (TAPB) and 2,5-bis(methylthio)terephthalaldehyde (BMTTPA)	Hg^{2+}	Adsorption/removal	[16]
DhaTG$_{Cl}$	2,5-Dihydroxyterephthalaldehyde (Dha) and triaminoguanidinium chloride (TG$_{Cl}$)	TcO_4^-	Adsorption/removal	[24]
BT-DG$_{Cl}$	1,3,5-triformylbenzene (Tb) and diaminoguanidinium chloride (DG$_{Cl}$)	Cr(VI)	Adsorption/removal	[25]
DhaTab-PBA	2,5-Diallyloxyterephthalaldehyde (Da-V), TAPB, and 4-mercaptophenylboronic acid (4-MPBA)	Catechol	Adsorption/removal	[28]
COF-S-SH	2,5-Divinylterephthalaldehyde (Dva), TAPB, and ethane-1,2-dithiol	Hg^{2+}	Adsorption/removal	[29]
JUC-570	3,3″,5,5″-Tetraisopropyl-2′,5′-bis((methylthio)methyl)-[1,1′:4′,1″-terphenyl]-4,4″-diamine (TBTD) and tetrakis(4-formylphenyl)silane (TFS)	Hg^{2+}	Adsorption/removal	[32]
3D-ionic-COF-1, 3D-ionic-COF-2	TFPM, diimidium bromide (DB) or ethidium bromide (EB)	MnO_4^-, anionic dye pollutants	Adsorption/removal	[33]
SCU-COF-1	2,4,6-Trihydroxybenzene-1,3,5-tricarbaldehyde (Tp), and aminated viologen (Viologen-NH$_2$)	$^{99}TcO_4^-$	Adsorption/removal	[34]
TFPT-TG$_{Cl}$-iCOF, 3D-COOH-COF	2,4,6-Tris(4-formylphenyl)-1,3,5-triazine (TFPT), and TG$_{Cl}$ Tetrakis(4-formylphenyl)methane (TFPM), and 3,3′-dihydroxybenzidine (DHBD)	2,4-dichlorophenol lanthanide ions	Adsorption/removal Adsorption/removal	[45] [50]
SIOC−COF-7	4,4″-bis(bis(4formylphenyl)amino)-[1,1′:4′,1″-terphenyl]-2′,5′-dicarbaldehyde (BFATD), and p-phenylenediamine (Pa)	iodine	Adsorption/removal	[56]
NDA-TN-AO	Naphthalene-2,6-dicarbaldehyde (NDA) and 2,2′,2″-(benzene-1,3,5-triyl)triacetonitrile (TN)	U^{IV}	Adsorption/removal	[59]
JNU-1	4,4′-biphenyldicarboxaldehyde (BPDA), 4,4′,4″-(1,3,5-triazine-2,4,6-triyl)tria-niline (Tz), and terephthaloyl chloride	Au (III)	SPE	[46]
CTpBD	Tp, benzidine (BD), diglycolic anhydride	Metal ions	online SPE	[26]
TAPB-DMTP-COFs	2,5-dimethoxyterephthalaldehyde (Dma) and TAPB	Anti-inflammatory drugs, phenols, iodine	stir bar sorptive SPE/SPME/Sensing	[60−63]
TpPa-1	Tp and Pa	Polycyclic aromatic hydrocarbons (PAHs)	MSPE	[64]
TpBD	Tp and BD	PAHs, and bisphenol chemicals	MSPE/HPLC/GC/	[47,65,66]
TFPB-BD	1,3,5-tris(4-formylphenyl)benzene (TFPB) and BD	Polychlorinated biphenyls	SPME	[41]
CTpPa-1	Tp, Pa and (+)-diacetyl-L-tartaric anhydride	Aromatic enantiomers	GC	[37]
COF-300	Terephthalaldehyde (Ta), and TAM	Aromatic compounds and isomers	HPLC/CEC	[51,67]
TpPa-MA	Tp, methacrylic anhydride (MA), and Pa	Anti-inflammatory drugs	HPLC	[68]
3D-IL-COF-1	TFPM and Pa	PAHs isomer	HPLC	[52]
(R-R)-CCOF 5	TAM and 1,3-dioxolane-4,5-dimethanols (TADDOL)	Alcohol enantiomers	HPLC	[39]
COF 1	Pyromelliticaciddianhydride (PMDA), and Tz	Ofloxacin enantiomer	HPLC	[40]
N$_0$−COF	TFPB and hydrazine	Bisphenols	CEC	[69]
Py-Azine COF	1,3,6,8-Tetrakis(4-formylphenyl)pyrene (TFPPy) and hydrazine	2,4,6-trinitrophenol (TNP)	Sensing	[43]
COF-BABD-DB	4′-(Bis(4-formylphenyl)amino)-[1,10-biphenyl]-3,5-dicarbaldehyde (BABD) and Pa	TNP	Sensing	[58]
TzDa	Tz and Dha	Metal ions	Sensing	[70]
TFPT-BTAN-AO	TFPT, 2,2′,2″-(benzene-1,3,5-triyl)triacetonitrile (BTAN), NH$_2$OH·HCl	UO_2^{2+}	Sensing	[35]
Py-TPE-COF	1,3,6,8-Tetrakis(4-aminophenyl)-pyrene (PyTTA), and 1,1,2,2-Tetrakis(4-formylphenyl)ethane (TPE-4CHO)	TNP	Sensing	[42]
TPE-Ph COF	Tetraphenylethene (TPE)-cored boronic acids (TPEBA), and 1,2,4,5-tetrahydroxybenzene (THB)	Ammonia	Sensing	[49]
COF-LZU8	2,5-bis(3-(ethylthio)propoxy)terephthalohydrazide (BTTA) and Tb	Hg^{2+}	Sensing	[30]
PTAzo	TFPT and 4, 4′-azodianiline (Azo)	Hg^{2+}	Sensing	[27]
TFPPy-DETHz-COF	TFPPy and 2,5-diethoxyterephthalohydrazide (DETHz)	Fluoride anion	Sensing	[71]
COF-CB	Dha, TAPB and 9-(4-Bromobutyl)-9H-carbazole	Pb^{2+}	Sensing	[72]
CCOF 7	6,6′-dichloro-2,2′diethoxy-1,1′-binaphthyl-4,4′-dialdehyde (BINOL-DA) and tris(4-aminophenyl)benzene derivative (TPE-TAM)	Terpene flavor molecules	Sensing	[38]

The hard-soft-acid-base principle reveals the extreme stable complexes can be formed with a hard acid and a hard base, or a soft acid and a soft base [74]. Introducing chelating soft base groups can efficiently promote the interaction of COFs with soft acids of heavy metal ions. Therefore, a series of sulfur (soft base) functionalized COFs were prepared to remove the soft acid of Hg^{2+} from the environment based on the chelation of S and Hg [16,29−31]. 1,2-ethanedithiol modified COF (COF-S-SH) was also synthesized for efficient adsorption/removal of Hg^{2+} (Fig. 3a). Compared with COFs without −SH, COF-S-SH exhibited better selectivity and stronger affinity for Hg^{2+}. The adsorption capacity of COF-S-SH for Hg^{2+} and Hg^0 reached 1350 mg g^{-1} and 863 mg g^{-1}, respectively (Fig. 3c)

[29]. Considering the harsh adsorption conditions of Hg and the entanglement of the sulphide with long chain, Huang et al. further synthesized a stable methyl sulfide functionalized COF (TAPB-BMTTPA-COF) with short sulfide chain to improve the efficiency for removal of Hg^{2+} (Fig. 3b) [16]. The methyl sulfide not only promoted the stability of imine-linked COFs with resonance effect, but also provided a high sulfur content and facilitated the exposure of active sites. TAPB-BMTTPA-COF achieved excellent performance for removal of Hg^{2+}. The concentration of Hg^{2+} decreased from 10 ppm to 0.01 ppm after 15 min adsorption with TAPB-BMTTPA-COF. The adsorption capacity of TAPB-BMTTPA-COF for Hg^{2+} (734 mg g^{-1}) was also much higher than those of many other porous materials
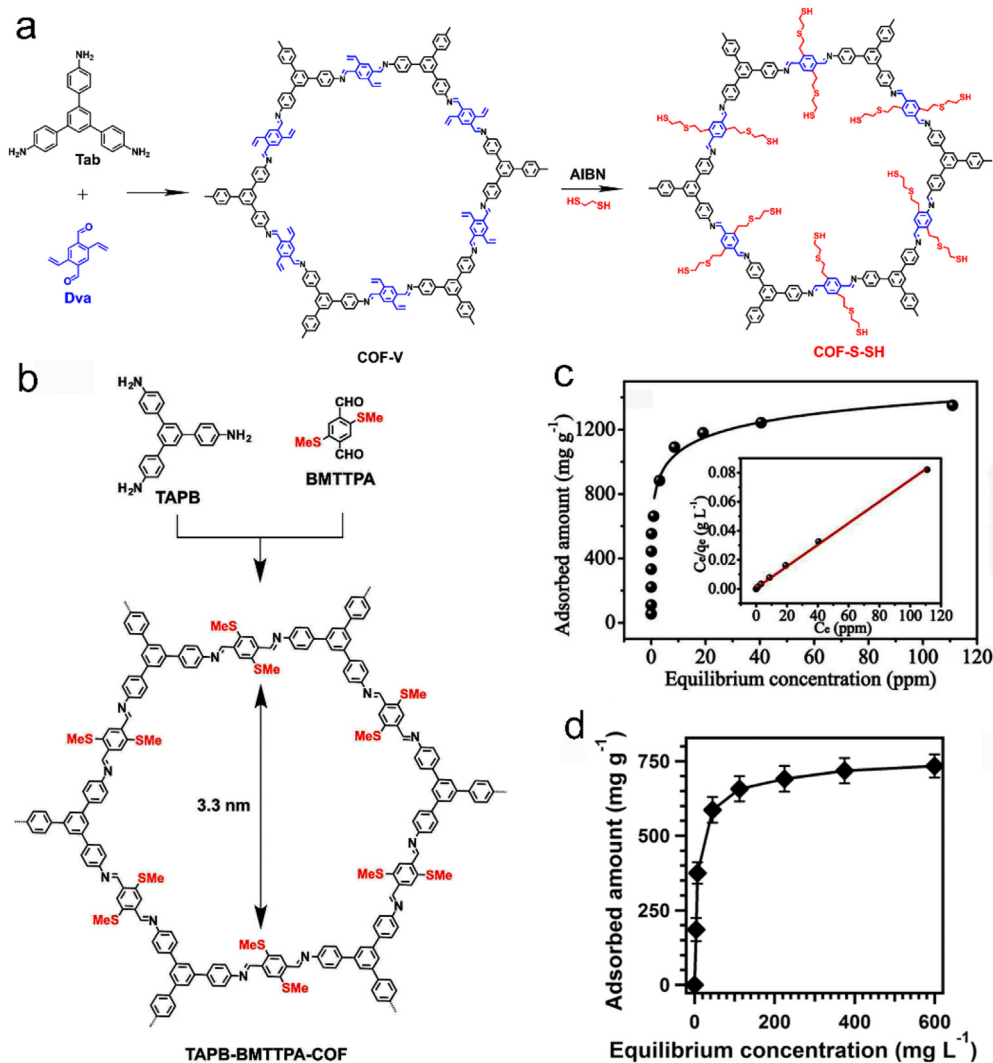
Fig. 3. Preparation of (a) COF−V, COF-S-SH and (b) TAPB-BMTTPA-COF for the adsorption/removal of Hg^{2+}. Hg^{2+} adsorption isotherms for (c) COF-S-SH and (d) TAPB-BMTTPA-COF (Reprinted with permission from ref. 16 and 29. Copyright 2017 American Chemical Society).

(Fig. 3d). In addition to 2D COFs, 3D COFs with rich pore channels are also promising adsorbents for adsorption/removal of pollutants. Thioether-functionalized 3D COFs JUC-570 and JUC-571 were prepared via bottom-up approach for efficient adsorption of Hg^{2+} with high absorption capacity (972 mg g^{-1} and 970 mg g^{-1}, respectively), rapid kinetics and favorable selectivity [32]. Additionally, lots of COFs such as BT-DG$_{cl}$, TbBD, COF-616 (consisting of ETTA and *p*-terphenyl-2',5'-dicarboxylic acid-4,4''-dicarboxaldehyde) and 3D-COOH-COF were also prepared as adsorbents by introducing the corresponding chelate groups in structure to apply in the adsorption/removal of Cr, Pb, Cu, Nd and lanthanide ions [25,50,75−77].

The employment of ionic units to construct ionic covalent organic frameworks (iCOFs) brings COFs rich ion exchange and electrostatic interaction with analytes. However, the strong charge repulsion between adjacent layers can lead to low crystallinity of iCOFs [78,79]. To overcome this problem, our group reported a knot-linker planarity control strategy for preparation of highly crystalline iCOFs, and further investigated the effect of crystallinity on the adsorption performance of iCOFs. Careful regulation of the structural planarity of monomers greatly improved the crystallinity of the prepared iCOFs, thereby facilitating the exposure of more active sites for adsorption [45]. The excellent ion exchange of COFs gives the iCOFs high potential in adsorption/removal of radioactive

nuclear pollutants [80], our group explored the potential of iCOFs in the adsorption/removal of radioactive TcO_4^-. TG$_{Cl}$ was applied to condense with Dha to prepare advanced cationic covalent organic nanosheets DhaTG$_{Cl}$. The anion exchange from the guanidine and the hydrogen-bond interaction from the hydroxyl group allowed DhaTG$_{Cl}$ to quickly and selectively adsorb ReO_4^- (an analogue of radioactive TcO_4^-) with large capacity of 437 mg g^{-1} (Fig. 4) [24]. Wang group also reported the preparation of an advanced iCOF SCU-COF-1 for direct removal of $^{99}TcO_4^-$ under extreme conditions. The cationic SCU-COF-1 constructed by irreversible tautomerism of aminated viologen and 2,4,6-triformylphloroglucinol had good crystallinity, acid stability and radiation resistance. Due to the anion exchange between $^{99}TcO_4^-$ and Cl^-, the SCU-COF-1 gave an unprecedented adsorption capacity of 702.4 mg g^{-1} for $^{99}TcO_4^-$ and reached equilibrium within 1 min [34]. The positively charged 3D iCOFs of 3D-ionic-COF-1 and 3D-ionic-COF-2 were prepared with linear ion units and tetrahedral connectors as building blocks for rapid adsorption of MnO_4^- (analogue of pertechnetate), anionic methyl blue and methyl orange via the ion exchange and size exclusion effect [33]. Besides ion exchange, the electrostatic interaction was also explored for the adsorption/removal of environmental pollutants. Qiu et al. prepared various photocatalytic COFs (named NDA-TN-AO, BD-TN-AO and DHBD-TMT) for adsorption of
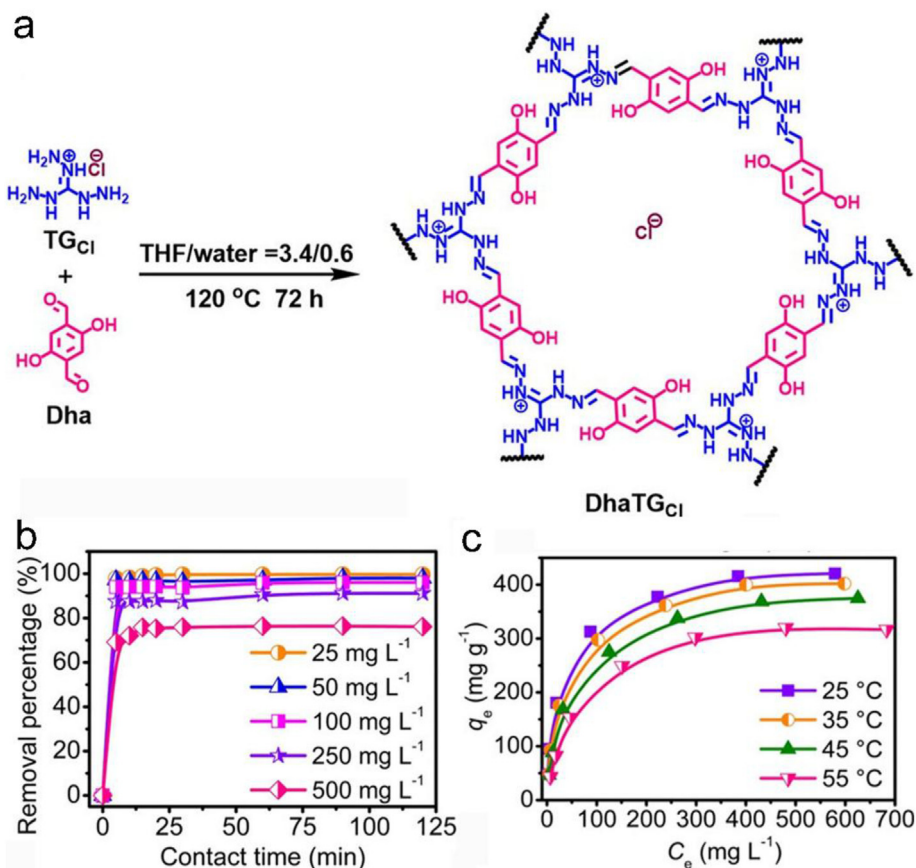
Fig. 4. (a) Preparation and structure of DhaTG$_{Cl}$. (b) Adsorption kinetics of DhaTG$_{Cl}$ for ReO$_4^-$ with different initial concentrations. (c) Adsorption isotherms of DhaTG$_{Cl}$ for ReO$_4^-$ (Reprinted with permission from ref. 24. Copyright 2019 American Chemical Society).
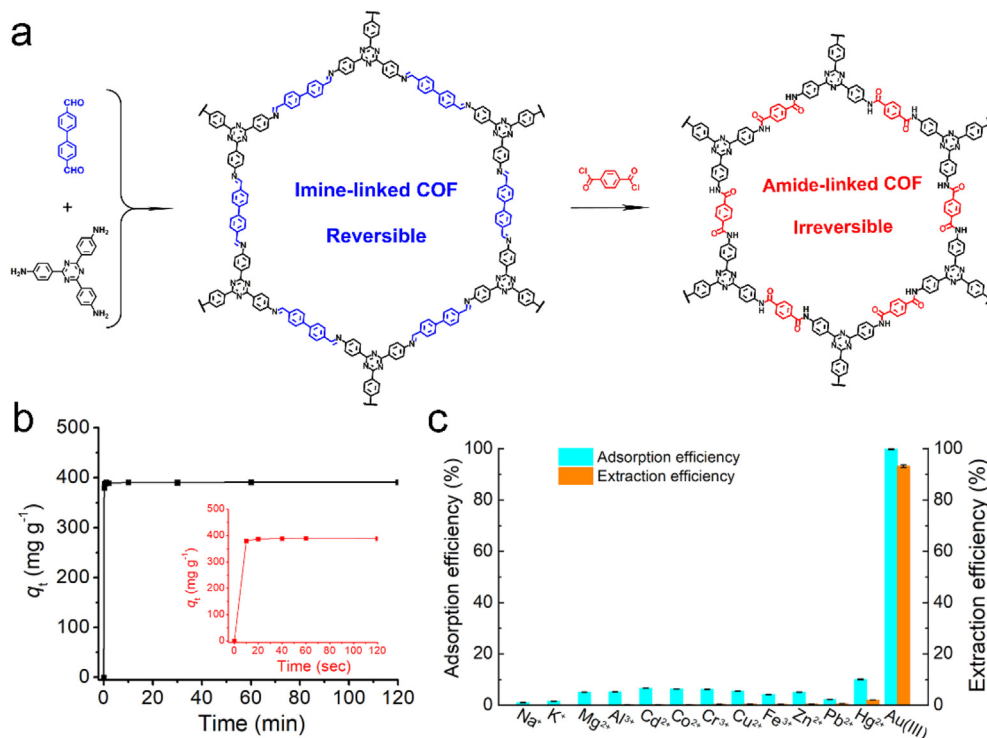
Fig. 5. (a) Preparation and structure of JNU-1. (b) Time-dependent adsorption of Au(III) on JNU-1. (c) Solid-phase dispersion extraction efficiency of Au(III) on JNU-1 in the presence of other interfering ions (Adapted with permission from ref. 46. Copyright 2020 John Wiley and Sons).
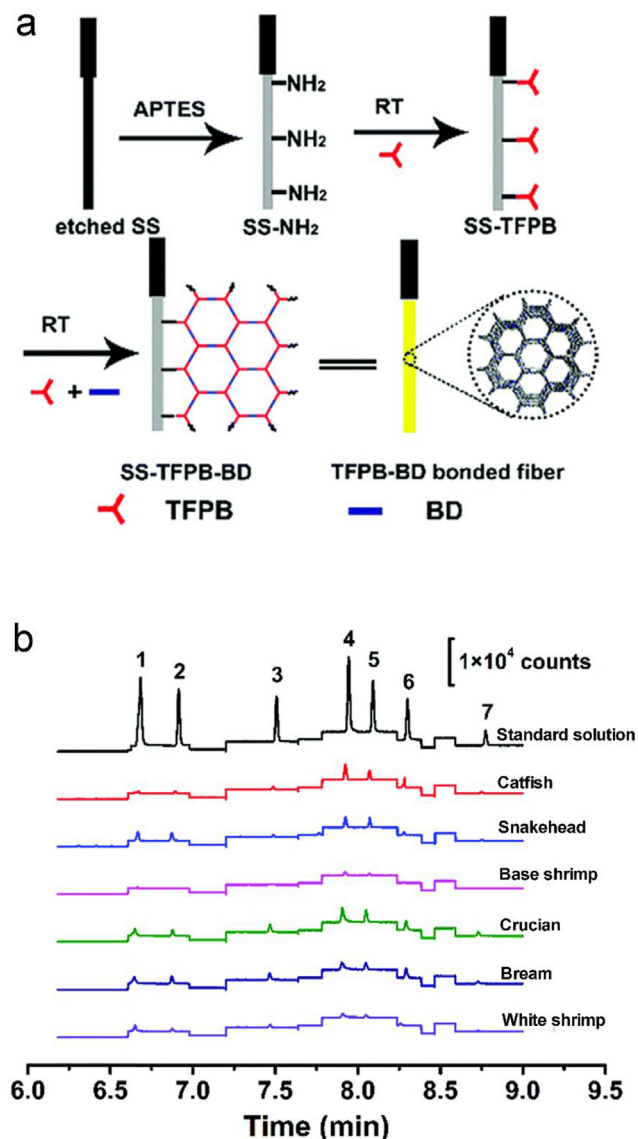
Fig. 6. (a) Illustration of in situ room-temperature preparation of the TFPB-BD bonded fiber. (b) GC/MS/MS chromatograms of PCBs in different samples after SPME with the prepared TFPB-BD bonded fiber. Peak identity: (1) PCB28, (2) PCB52, (3) PCB101, (4) PCB118, (5) PCB138, (6) PCB153 and (7) PCB180 (Reproduced from ref. 41 with permission from The Royal Society of Chemistry).

uranium. The U^{VI} can be reduced to U^{IV} by these photocatalytic COFs, and then the electrostatic interaction of U^{IV} and COFs further increased the capacity of uranium [36,59,81].

Heteroporous COFs with co-existing different types of pores endow them with hierarchical porosity, which weakens the diffusion barrier and facilitates the rapid capture of guest molecules. The multiple pores also render heteroporous COFs simultaneous adsorption of different sizes of molecules [82]. In a typical example, Yin et al. prepared heteropore COF SIOC−COF-7 with two different kinds of micropores as adsorbent [56]. The hierarchical porosity in conjunction with the cavity of the hollow microspheres and the well-ordered structure made SIOC−COF-7 able to capture volatile iodine (481 wt%). Karah et al. further fabricated four hierarchical 3D porous COF-foams with 2D COFs (TpPa-2, TpPa-NO₂, TpAzo, and TpBD-Me₂) through an in situ gas-phase foaming protocol [57]. The disordered 3D structure constructed from crystalline 2D COFs with ordered micropores allowed the pollutants to be quickly diffused,

resulting in ultra-fast adsorption. The 3D COF-foams could remove a variety of dyes and inorganic pollutants including rhodamine B, methylene blue, acid fuchsin, and rose bengal, iodine and $KMnO_4$ from water in 10 s with a removal efficiency of >95%.

3.2. Sample pretreatment

Sample pretreatment is crucial for the analysis of environmental sample due to the complexity of matrix and low concentration of targets [83]. COFs also exhibit great capacity in sample pretreatment including solid-phase extraction (SPE), solid-phase microextraction (SPME) and magnetic solid-phase extraction (MSPE).

To extract the target in complex matrix, the adsorbents in SPE should possess good selectivity and stability. Our group developed a building block exchange strategy to prepare irreversible amide-linked COF named JNU-1 for ultrafast dispersive solid-phase extraction of Au(III) (Fig. 5a). The introduction of irreversible amide linkage not only greatly improved the stability of JNU-1, but also rendered JNU-1 selective interaction with Au(III) through the hydrogen bonding of C−H⋯Cl and N−H⋯Cl in conjunction with the coordination of O and Au. Notably, JNU-1 could selectively adsorb 99.8% of Au(III) within 10 s. Even in the presence of the high concentration of potential competing metal ions (Na^+, K^+, Mg^{2+}, Al^{3+}, Cd^{2+}, Co^{2+}, Cr^{3+}, Cu^{2+}, Fe^{3+}, Zn^{2+} and Pb^{2+}), JNU-1 gave extraction efficiency of 93.2% for Au(III), but only 0.03−2.1% for the competing metal ions (Fig. 5b) [46]. Besides the direct dispersion of adsorbents with samples, COFs are also packed into a column for SPE to extract the analytes. Ji et al. prepared an amino-modified COF (NH_2@COF) as the adsorbent of SPE column for the enrichment of carboxylic acid pesticides with good selectivity. The developed NH_2@COF based SPE coupled with high performance liquid chromatography-photo-diode array detector (HPLC-DAD) gave low detection limits (LODs, 0.04−0.20 ng mL^{-1}), wide linear ranges (0.2−100 ng mL^{-1}) and good recoveries (89.6%−102.4%) for six carboxylic acid pesticides in water [84]. COFs are also coated onto stir bar to develop stir bar sorptive SPE. The TAPB-DMTP-COFs coated stir bar was prepared to effectively detect anti-inflammatory drugs in environmental water samples with low LODs (0.039−0.312 μg L^{-1}) and wide linear range (0.2/1−500 μg L^{-1}) [60]. As online SPE is automatable, easy to operate and effective to avoid artificial error, Liu et al. used CTpBD as an online SPE adsorbent for the pre-enrichment of trace metals in complex samples [26]. Combining with inductively coupled plasma mass spectrometry gave the LODs of 2.1−21.6 ng L^{-1} and the linear range of 0.05−25 μg L^{-1} for heavy metal ions.

SPME integrates the sampling, extraction, concentration, and injection, showing wide application in environmental analysis [85]. The key role of COFs in SPME is the preparation of COFs based SPME fiber. As conventional physical adhesive method leads to low stability and durability of the fiber, our group developed a room-temperature in situ preparation of COF TFPB-BD bonded fiber for the determination of polychlorinated biphenyls (PCBs) (Fig. 6a) [41]. The covalent bonding method significantly improved the stability of the fiber. The developed SPME-gas chromatography -tandem mass spectrometry (GC-MS/MS) method based on TFPB-BD fiber for PCBs exhibited low LODs (0.07−0.35 ng L^{-1}), high enhancement factors (4471−7488), and good recoveries of 87.1−99.7%, indicating the great potentials of COFs in SPME (Fig. 6b) [41]. Jia et al. reported the utilization of polydopamine (PDA) as a linking agent to immobilize a hydrazone COF (consisting of Tb and terephthalic dihydrazide) onto stainless steel wire. The π-π interaction, hydrogen bonding, hydrophobicity, and van der Waals interactions of the hydrazone COF allowed the prepared SPME fiber to selectively extract pyrethroids with enhancement factors of 307−2327. The COF-PDA fiber coupled with GC-electron capture
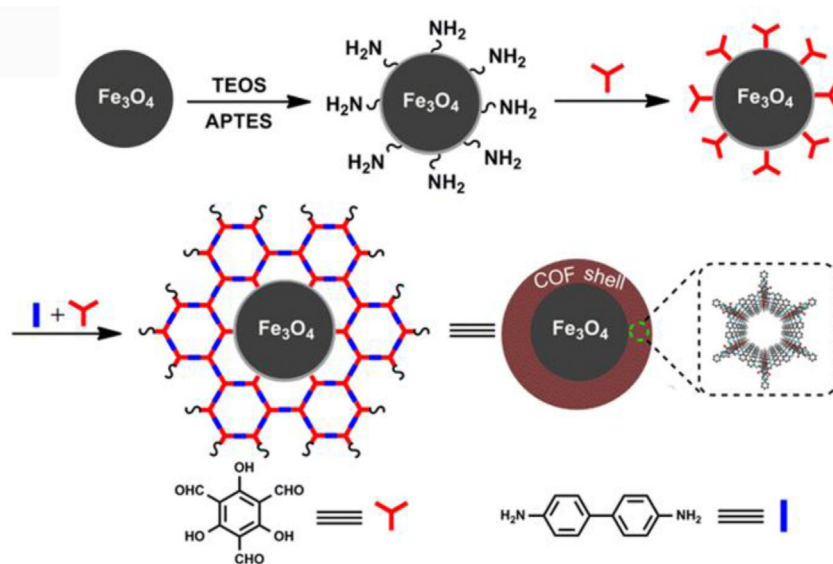
Fig. 7. Illustration for a monomer-mediated in situ growth synthesis of Fe$_3$O$_4$@TpBD composites with core-shell structure (Reproduced from ref. 65 with permission from The Royal Society of Chemistry).

detector showed low LODs (0.11−0.23 μg kg^{-1}) and good precision (3.6−12.1%RSD) for pyrethroids [86]. Additionally, the COF TPB-DMTP coated fiber coupled with GC-MS was also prepared via room-temperature growth for the extraction of ultra-trace poly-brominated diphenyl ethers (PBDEs) and phenols in water with low LODs (0.0083−0.0190 ng L^{-1} for PBDEs and 0.0048−0.015 ng L^{-1} for phenols) and wide linear range (0.05−100 ng L^{-1} for PBDEs, and 0.05−1000 ng L^{-1} for phenols) [61,62].

MSPE attracts great concerns due to its great convenience. The essential part for MSPE is the preparation of magnetic adsorbents [87]. Our group developed a monomer-mediated in situ growth method to prepare magnetic COF Fe$_3$O$_4$@TpBD with a controllable core-shell structure for MSPE of a typical class of endocrine-disrupting chemicals bisphenols in water (Fig. 7). The prepared Fe$_3$O$_4$@TpBD composites possessed the adsorption capacities of 160.6 and 236.7 mg g^{-1} for bisphenol A (BPA) and bisphenol AF (BPAF), respectively. The integration of magnetic separation and various interactions of π-π interaction and hydrogen bonding gave the Fe$_3$O$_4$@TpBD simple and fast extraction of bisphenols [65]. Compared with the core-shell magnetic COFs composite, a novel bouquet-shaped magnetic COFs composite with higher proportion of COFs can give higher adsorption performance. The developed MSPE-HPLC method based on the bouquet-shaped magnetic TpPa-1@Fe$_3$O$_4$ exhibited low LODs (0.24−1.01 ng L^{-1}) and wide linear ranges (2.0−200.0 ng L^{-1}) for PAHs in water sample [64]. To increase selectivity, the amino group was introduced into the magnetic COF consisting of TAPB and Ta to form the Fe$_3$O$_4$@[NH$_2$]-COFs. The introduction of amino groups can bring the COFs hydrophobic and electrostatic interactions for the perfluoroalkyl acids (PFAAs). Combination of MSPE based on Fe$_3$O$_4$@[NH$_2$]-COFs with HPLC-MS/MS gave low LODs (0.05−0.38 ng L^{-1}) and wide linear ranges (10−10,000 ng L^{-1}) for PFAAs in real water samples [88].

3.3. Chromatographic separation

As the most effective separation technology, the chromatography including high performance liquid chromatography (HPLC) and gas chromatography (GC) is widely applied in environmental analysis. The stationary phase of chromatography is dominant for

separation performance [89]. Various unique properties including rich noncovalent interactions, great stability, and tunable pore chemistry make COFs ideal candidates as stationary phase for chromatography [90]. Our group proposed a simple room temperature solution phase approach for preparing a spherical TpBD with good stability and large surface area (Fig. 8a). We further synthesized a TpBD-coated capillary column by a dynamic coating method and explored the potential of the prepared column in GC. Owing to the van der Waals, π-π and hydrogen bonding interactions between TpBD and the analytes, the TpBD-coated capillary column gave higher resolution for the separation of many industrial contaminants than commercial HP-5 capillary column (Fig. 8b), indicating the great potential of COFs as the stationary phase in GC [47]. To enhance the stability of GC column, we further developed a covalent bonding approach for the preparation of three chiral COFs (CTpPa-1, CTpPa-2 and CTpBD) bonded capillary columns to expand COFs to chiral GC separation. The prepared columns enabled baseline-separation of four chiral compounds in 6 min (Fig. 8c and d), with better resolution than commercial β-DEX 225 and Cyclosil B chiral capillary columns [37].

The irregular shape, sub-micron size and wide size distribution of COFs particles are the main barriers for the application of COFs as the stationary phase for HPLC. The preparation of uniformly spherical COF@silica composites is an efficient way to address the above limitation. In this direction, we reported a simple in-situ growth method to prepare a uniform and controllable COF-shell-SiO$_2$-core composite (TpBD@SiO$_2$) as the stationary phase for HPLC [66]. The prepared TpBD@SiO$_2$ packed columns gave the baseline separation of different probe molecules including toluene, ethyl-benzene, PAHs and RP-5 (theophyline, anisole, methyl benzoate, p-nitro-aniline, and o-xylene). Subsequently, we further developed a layer-by-layer method for the grafting of 3D COF on the surface of SiO$_2$ to resolve the difficult separation of the excess COFs from the COF@SiO$_2$ composite (Fig. 9a). The prepared COF-300@SiO$_2$ in this way was explored as the stationary phase in HPLC and exhibited a reversed-phase separation mechanism and moderate hydrophobicity. COF-300@SiO$_2$ gave baseline separation of position isomers with high column efficiency (39,591 plates m^{-1} for p-nitrophenol)
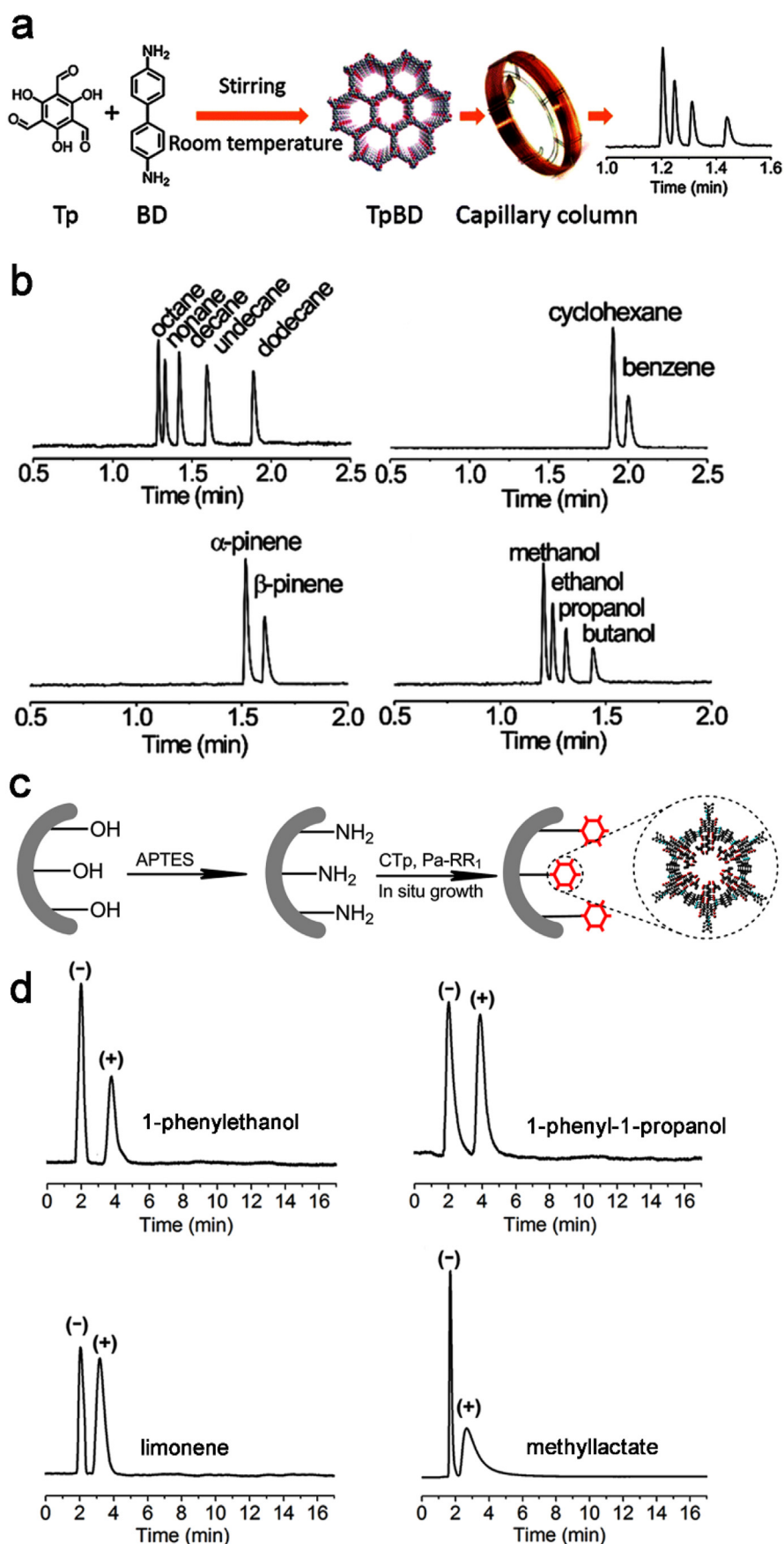
Fig. 8. (a) Preparation of TpBD-coated capillary. (b) GC chromatograms of alkanes, cyclohexane and benzene, α-pinene and β-pinene, and alcohols on TpBD-coated capillary (Reproduced from ref. 47 with permission from the Royal Society of Chemistry). (c) Synthesis of chiral COFs-bound capillary. (d) Gas separation chromatograms of 1-phenylethanol, 1-phenyl-1-propanol, limonene, and methyl lactate on CTpPa-1 bound capillary (Adapted with permission from Ref. 37. Copyright 2016 Springer Nature).
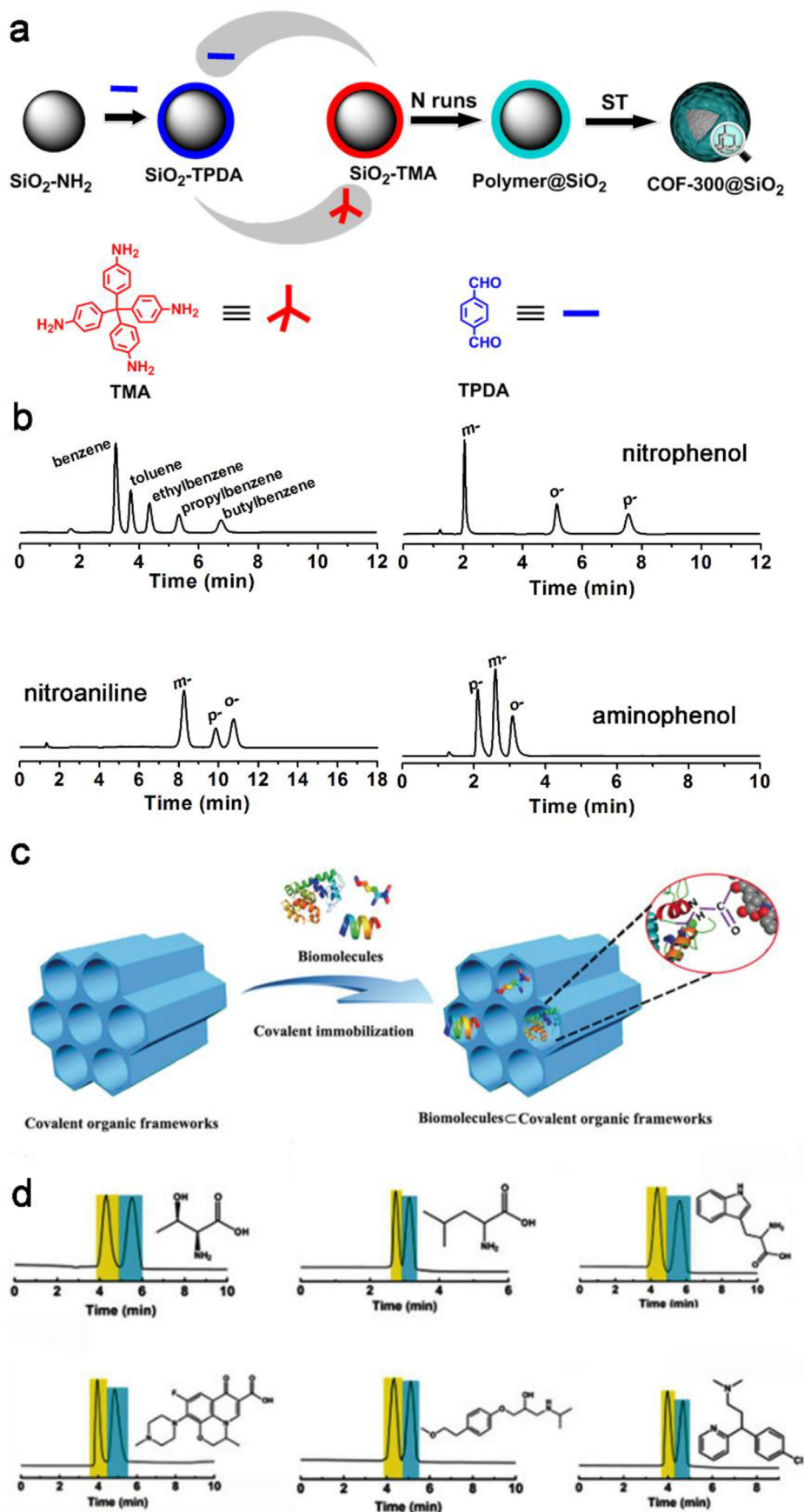
Fig. 9. (a) Layer-by-layer preparation of COF-300@SiO₂ as HPLC stationary phase. (b) HPLC separation chromatograms of benzene homologue and isomers on the COF-300@SiO₂ packed column (Reproduced from ref. 51 with permission from the Royal Society of Chemistry). (c) Covalent immobilization of biomolecules into COFs. (d) chiral HPLC separation chromatograms of threonine, leucine, tryptophan, ofloxacin, metoprolol, and chlorpheniramine on lysozyme⊂COF 1 (Reproduced with permission from ref. 40. Copyright 2018, John Wiley and Sons).
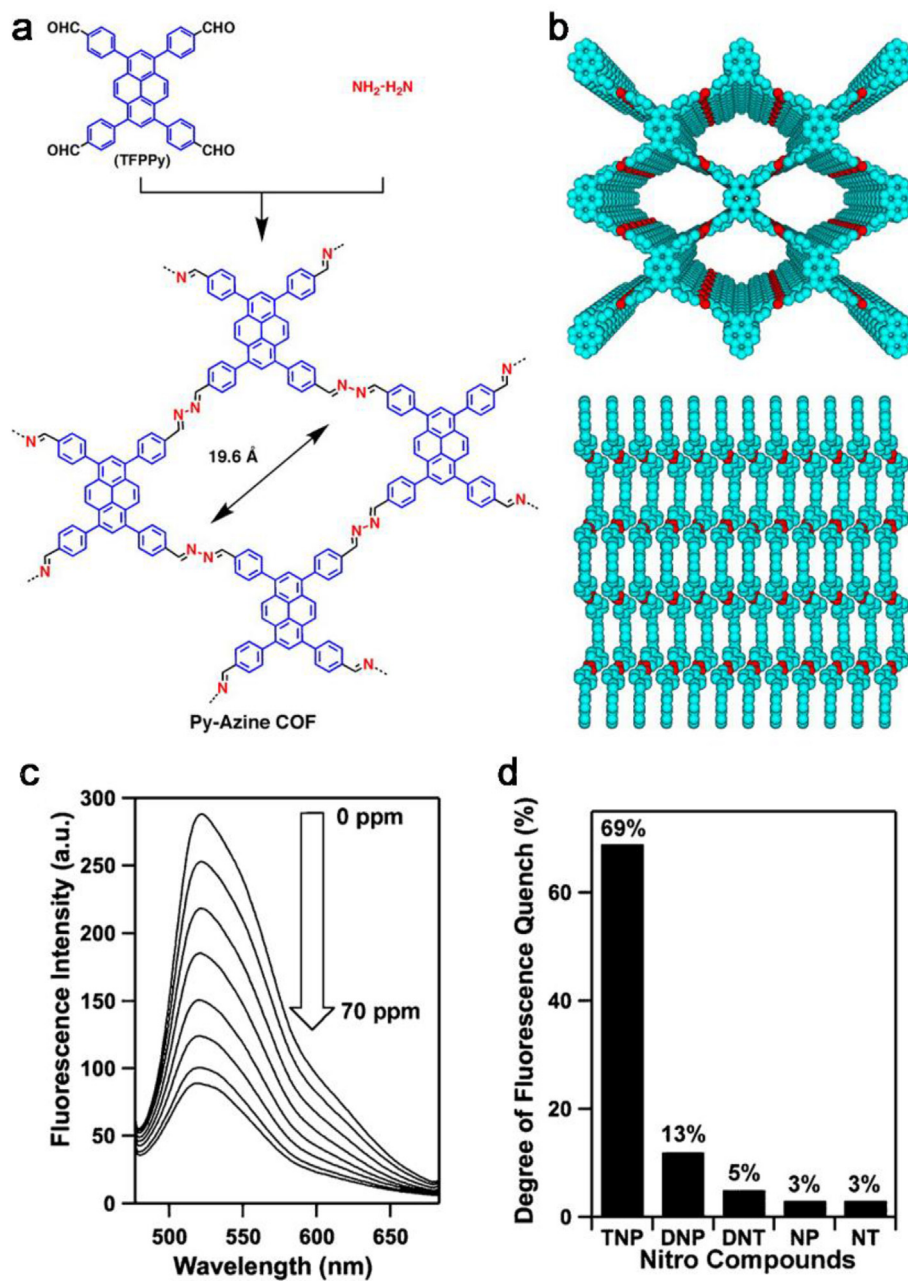
Fig. 10. (a) Preparation and structure of Py-Azine COF. (b) Top and side Views of the AA stacking structure of Py-Azine COF. (c) Fluorescence quenching of Py-Azine COF with TNP (0–70 ppm) in acetonitrile. (d) Degree of fluorescence quenching with 70 ppm different nitro compounds (Reprinted with permission from ref. 43. Copyright 2013 American Chemical Society).

and good accuracy (Fig. 9b) [51]. Our work reveals the excellent capability of 3D COF for the separation of isomers.

The preparation of COF-monolith is another way to explore COFs as the stationary phase for HPLC. Our group developed a bottom-up approach to prepare TpPa-MA-co-EDMA monolithic column for HPLC [68]. The prepared monolithic column possessed good uniformity and permeability, and gave high resolution for the separation of acidic and alkaline substances as well as organic pollutants such as PAHs, anilines and phenols. To show the potential of 3D COFs in HPLC, a 3D COF 3D-IL-COF-1 monolithic column was further prepared via facile incorporating 3D-IL-COF-1 into monolith. The uniform structure, good permeability, and high

mechanical stability of the prepared 3D-IL-COF-1 monolithic column not only made it promising for broad-spectrum chromatographic separation of neutral, acidic, and basic compounds, but also rendered it better separation of isomers than a C18 column [52].

The preparation of chiral COFs as the stationary phase for HPLC also draws great concern [91]. The imine-linked 3D COFs (R-R)-CCOF 5 and (R-R)-CCOF 6 were prepared through the condensation reaction of tetrahedral tetra(4-anilyl)methane and chiral tetraaldehyde with better stability and crystallinity. The 3D CCOFs had a 4-fold interpenetrating network structure and chiral dihydroxy-modified tubular channels. The (R-R)-CCOF 5 and (R-R)-CCOF 6 packed columns showed good HPLC separation performance of

racemic alcohol [39]. In addition to the synthesis of chiral COFs with the chiral building blocks, Zhang et al. reported a method for covalently anchoring chiral biomolecules (such as amino acids, peptides and enzymes) into COFs to introduce chirality (Fig. 9c) [40]. The chiral separation ability of biomolecules⊂COF mainly derived from the specific interaction between biomolecules and racemates. The lysozyme⊂COF 1 was used for HPLC stationary phase, and exhibited good separation of various racemates in both normal and reverse phase (Fig. 9d).

Electrochromatographic (CEC), a combination of HPLC and electrophoresis, shows great potential in separation. An azine-linked COF (N_0−COF) consisting of TFPB and hydrate was successfully coated onto the capillaries for CEC separation of bisphenol compounds (BPs). This method had good resolution (linear ranges were 5−100 $\mu g\ mL^{-1}$, LODs were 0.91−2.81 $\mu g\ mL^{-1}$) and high theoretical plates (58.78−107.50 plates m^{-1}) in real samples [69]. Niu reported the in-situ growth of 3D COFs-capillary for CEC. The hydrophobic interaction and size selection interaction dominated the separation of five groups of aromatic compounds [67]. Recently,

COFs were further applied in CEC-MS. The spherical COF−V was prepared from TAPB and Dva, and further applied to modify capillary column for CEC-MS analysis of alkylbenzene, chlorobenzene and phenolic compounds with good repeatability and stability [92].

3.4. Sensing

Fluorescent COFs are potential sensors for the detection of pollutants. The interaction between the guest molecules and COFs may lead to fluorescence quenching or enhancement, which can realize visual observation or spectral detection of various analytes [93]. Jiang and co-workers firstly reported an azine-Linked COF (Py-Azine COF) (Fig. 10a and b) as a chemosensor for highly selective sensing of 2,4,6-trinitrophenol (TNP) [43]. The pyrene units at the vertices and the azine linkers on the edges gave remarkable fluorescence and unique chemosensing property of Py-Azine COF. TNP could selectively and sensitively quench the fluorescence of Py-Azine COF. The quenching constant was $9.8 \times 10^{13}\ M^{-1}\ s^{-1}$,
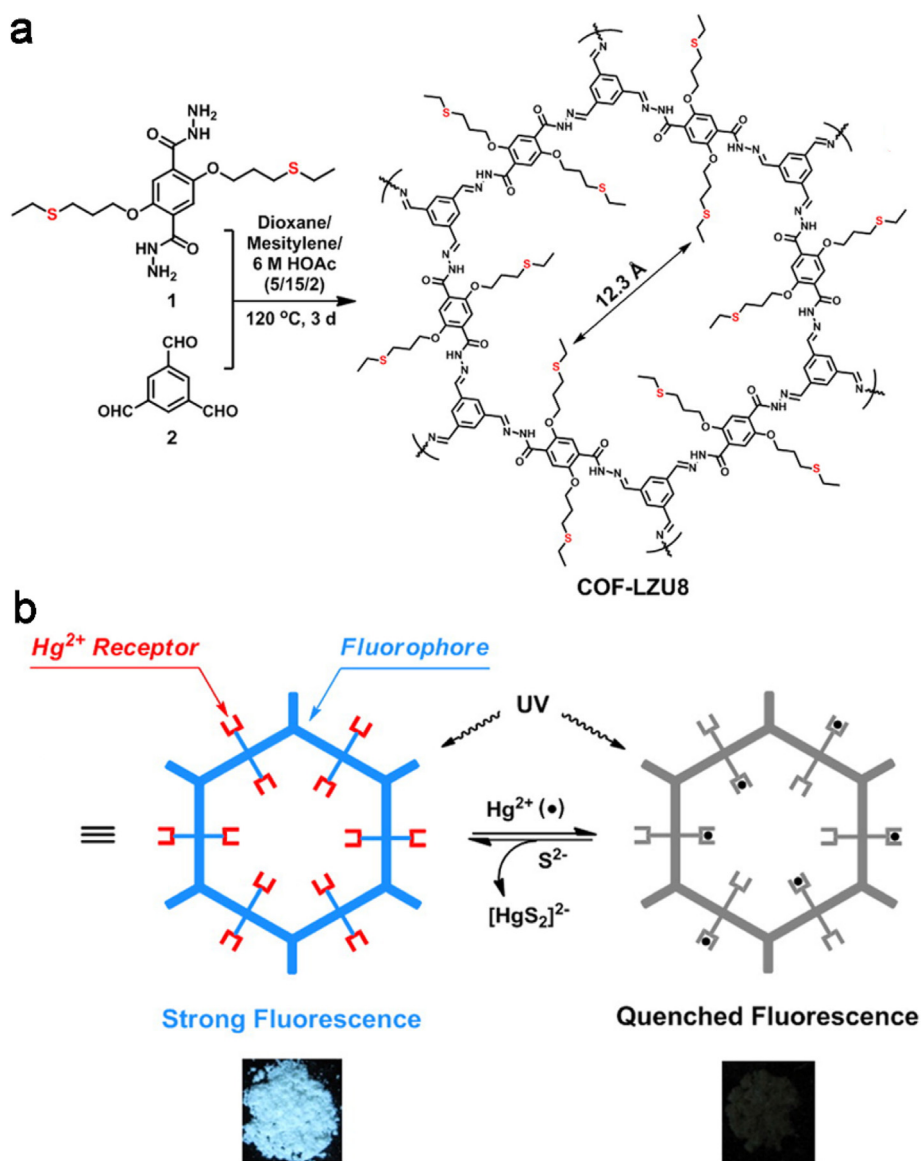
Fig. 11. (a) Synthesis and structure of COF-LZU8. (b) Illustration of the sensing of Hg^{2+} with COF-LZU8. (Reprinted with permission from ref. 30. Copyright 2016 American Chemical Society).
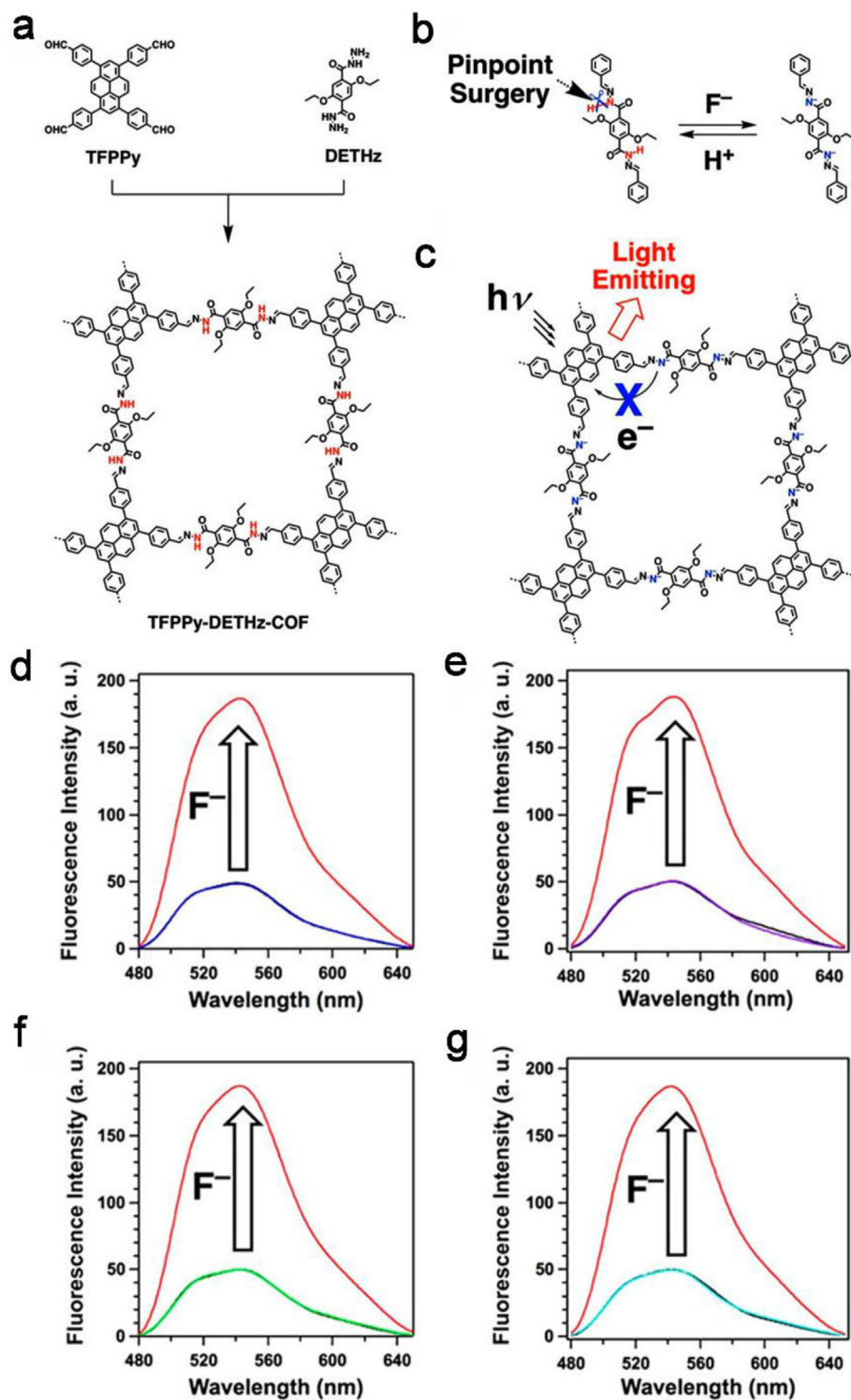
Fig. 12. (a) Preparation and structure of TFPPy-DETHz-COF. (b) Pinpoint surgery on the N–H unit of the hydrazone linkage that undergoes acid–base reaction with F⁻ and its regeneration with acid; (c) Fluorescence turn-on mechanism of TFPPy-DETHz-COF. (d–g) Fluorescence change of TFPPy-DETHz-COF with addition of (d) Cl⁻, (e) Br⁻, (f) I⁻, and (g) NO_3^- followed by addition of F⁻ (Reprinted with permission from ref. 71. Copyright 2018 American Chemical Society).

three-orders-of-magnitude higher than those of conventional bimolecular quenching systems (Fig. 10c and d). Zhu et al. also reported two fluorescent heteropore COFs (COF-BABD-BZ and COF-BABD-DB) for selective sensing of TNP [58]. The fluorescence of the two dual-pore COFs with uncommon staggered stacking structure was selectively quenched by TNP among various nitroaromatic analytes. The Stern–Völmer quenching constants were 4.5×10^5 M^{-1} for COF-BABD-BZ and 5.7×10^5 M^{-1} for COF-BABD-DB, respectively. Moreover, the two COFs further served as rapid naked-eye sensors for detecting TNP. Our group explored the potential of four COFs (TaTa, DhaTab, TRITER-1 and TzDa) in selectively sensing of Fe^{3+}. DhaTab exhibited the most sensitive

response to Fe^{3+} and its quenching coefficient was 1×10^5 M^{-1}. DhaTab was further applied as sensor for sensitive detection of Fe^{3+} in water with a wide linear range of 5−500 μM and the LOD of 0.12 μM [70]. Qiu et al. also synthesized TFPT-BTAN-AO with fluorescent properties for the selective and sensitive (LOD of 6.7 nM) detection of UO_2^{2+} in aqueous solutions based on the strong interaction between UO_2^{2+} and the amidoxime sites of TFPT-BTAN-AO [35].

In order to eliminate the aggregation-caused quenching (ACQ) of COF layers, several strategies were developed. Gao et al. synthesized a sub-micron spherical COF (Py-TPE-COF) as chemical sensor for sensitive (up to ppm level) and selective detection of TNP with high photoluminescence via the reaction of PyTTA and TPE-4CHO. The application of non-planar TPE and the fabrication of COFs into spherical particles reduced the π-π stacking of the COF layer, leading to the efficient inhabitation of the fluorescence quenching effect [42]. Jiang group reported another approach via the introduction of the aggregation-induced emission (AIE) mechanism to prepare a highly luminescent boronate ester-linked COF (TPE-Ph COF) with AIE-active TPEBA and THB as building units. Considering that the boronate linkages in TPE-Ph COF could interact with ammonia (Lewis acid−base), TPE-Ph COF was further developed as a sensor for reporting ammonia at sub ppm level [49].

Specific receptors are always introduced into COFs structure to promote selectivity for sensing more analytes. Ding et al. integrated the thioether group into the fluorescence COF framework to prepare COF-LZU8 as the Hg^{2+} receptor for the detection Hg^{2+} (Fig. 11). The fluorescence of COF-LZU8 was effectively quenched by Hg^{2+}, allowing COF-LZU8 for highly sensitive and selective sensing of Hg^{2+} (Fig. 11) [30]. Similarly, Zhao et al. used p-diethylnylbenzene to modify TPB-DMTP-COF consisting of TAPB and 2,5-dimethoxyterephthalaldehyde (DMTA) to obtain a chemically stable COF-PA containing quinoline and phenylacetylene units. The strong interaction of the quinoline and phenylacetylene units with iodine effectively quenched the fluorescence of COF-PA, allowing selective sensing of iodine [63].

Combination of COFs with other materials is also an attractive method to expand the sensing property of COFs. For example, our group prepared a gold nanoparticle (AuNPs) decorated imine-linked COF PTAzo [27]. In the presence of Hg^{2+}, PTAzo-AuNPs showed peroxidase activity to oxidize 3,3′,5,5′-tetramethylbenzidine from colourless to blue, thereby realizing the colorimetric detection of Hg^{2+}. The proposed method for the detection of Hg^{2+} had a wide linear range of 5−200 nM, low LOD of 0.75 nM and quantitative recovery of 97−104%. Yuan et al. directly grew COF films on interdigitated electrodes (IDEs) for the detection of capacitive benzene [31]. The dielectric constant of COF bonded IDEs varied with the concentration of the analyte. The developed COF-based sensor exhibited lower LOD (340 ng mL^{-1}), less power consumption and higher selectivity than some metal oxide semiconductors sensor for benzene.

Compared with the turn-off sensing, the turn-on sensing shows higher sensitivity. In a typical example, Li et al. developed a turn-on fluorescence sensing based on hydrazone-linked TFPPy-DETHz-COF for fluoride anion (Fig. 12a) [71]. The deprotonation activity of hydrazone eliminated the fluorescence quenching pathway, laying the foundation of the turn-on sensing. It was found that the deprotonation of N−H to N^- anion in TFPPy-DETHz-COF was only triggered by the F^- anion (Fig. 12b and c). The TFPPy-DETHz-COF based sensor gave the LOD down to 50.5 ppb for F^- without interference from Cl^-, Br^-, I^-, and NO_3^- (Fig. 12d−g). Zhang et al. also developed carbazole-grafted COF-CB for turn-on fluorescence sensing of Pb^{2+}. The coordination and charge transfer of Pb^{2+} with the nitrogen and oxygen atoms in COF-CB enhanced the fluorescence intensity, allowing COF-CB for highly selective detection of Pb^{2+} with the LOD of 1.48 μM [72].

Enantioselective sensing is expected to be a promising method for detecting and identifying enantiomers owing to the advantages of high sensitivity, low cost, and simple operation [94,95]. Wu
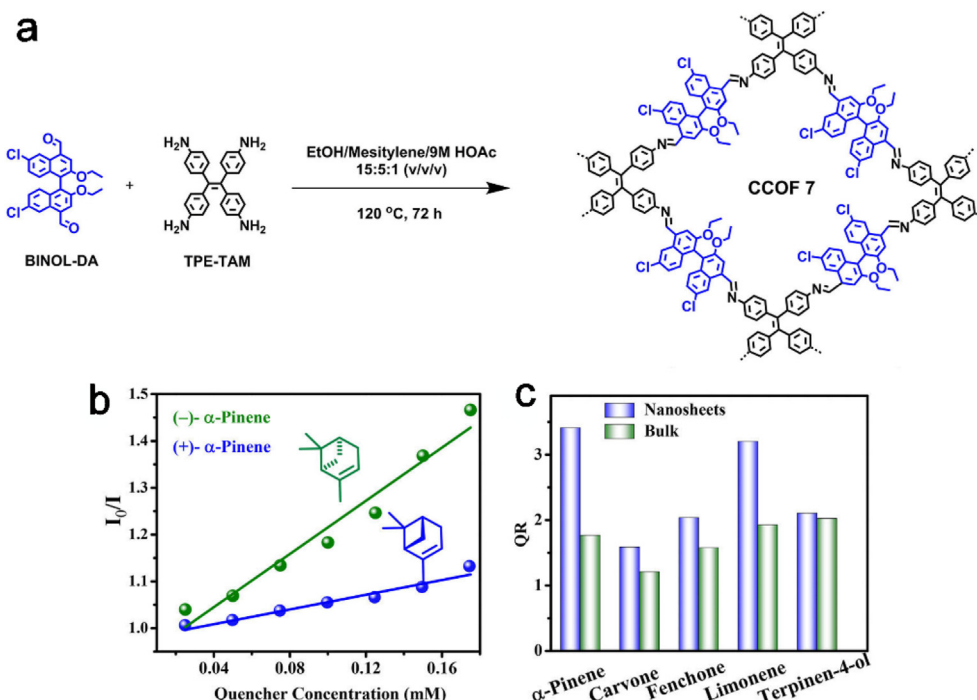
Fig. 13. (a) Preparation and structure of CCOF-7 nanosheet. (b) Stern−Völmer plots of CCOF-7 nanosheet upon addition of α-pinene in methyl cyanide. (c) Enantioselective quenching ratio for several terpenes. (Reprinted with permission from ref. 38. Copyright 2019 American Chemical Society).

et al. applied 1,1-bi-2-naphthol (BINOL) as the building block to synthesize a chiral COF (CCOF-7) and its 2D nanosheet with great fluorescence property for enantioselective sensing (Fig. 13a) [38]. Chiral odor vapors could quench the fluorescence of the 2D CCOF-7 nanosheet through the supramolecular interaction with the BINOL group, so that excellent chiral vapor sensors could be produced. In addition, its enantioselectivity was significantly improved due to the channel confinement effect and conformational rigidity of the BINOL site in 2D CCOF-7 nanosheet. In accordance with the linear Stern−Völmer equation, the measured fluorescence $[I_0/I]$ varied as a function of analyte concentration [M] in a linear relationship, realizing the chiral sensing of terpene flavor molecules (Fig. 13b).

4. Conclusion

We have highlighted recent progress on the design, preparation and application of advanced COFs for adsorption/removal, separation and sensing of typical environmental pollutants. The introduction of functionality in conjunction with the high surface area, permanent porosity and ordered crystalline structure allows COFs as excellent adsorbent and stationary phase to show fast adsorption kinetic, large adsorption capacity, high selectivity and excellent separation performance for various environmental contaminants including heavy metal ions, radionuclides, and toxic organic pollutants. The luminescent property and the extended π-conjugation framework make COFs excellent fluorophores for turn on/off sensing of pollutants. To meet the harsh analysis conditions of environmental samples, various available approaches are developed to improve the stability of COFs. Moreover, progress in synthetic chemistry, topological design and materials chemistry gives great structure evolution of COFs (from 2D to 3D and from single pore to hierarchical pore) to promote the performance of COFs in environmental analysis.

To date, COFs have shown great potential as candidate materials for environmental analysis owing to their high stability, accessible functionality, ordered porosity, and pre-designable structure. Nevertheless, the development of COFs in environmental analysis is still at a preliminary stage and several tough challenges remain to be solved.

As we know, the tunable functionality endows COFs with special properties to meet the demands of diverse applications. However, conventional strategies to introduce functional groups into the pore of COFs always give negative effect on the porous properties including crystallinity, surface area, and pore volume. Thus, it is hard to take full utilization of the complete pore of COFs. Additionally, the confined space of the pore goes against the accessibility of functional groups with the analytes. The employment of the linkage in COFs as functional moiety seems to be a promising way to reduce the above-mentioned negative effect.

Although various COFs with different structures have been applied in environmental analysis, the relationship of the COFs structure and their performance remains unclear. Future investigations should focus on the mechanisms of the structure-performance relationship for COFs in environmental analysis. The application of quantum mechanics and molecular dynamics is an effective way to explore the structure-performance relationship as well as the interaction mechanism of analyte and COFs.

Last but not least, the high synthetic cost and unknown environmental risk limit the mass production of COFs for practical applications in environmental analysis. The interdisciplinary corporation including synthetic chemistry, materials chemistry and environmental toxicology is indispensable in the future to promote the feasibility of COFs in practical environmental analysis.

Declaration of competing interest

The authors declare that they have no known competing financial interests or personal relationships that could have appeared to influence the work reported in this paper.

Acknowledgements

References

[1] A.P. Cote, A.I. Benin, N.W. Ockwig, M. O'Keeffe, A.J. Matzger, O.M. Yaghi, Science 310 (2005) 1166.
[2] X. Feng, X. Ding, D. Jiang, Chem. Soc. Rev. 41 (2012) 6010.
[3] S.Y. Ding, W. Wang, Chem. Soc. Rev. 42 (2013) 548.
[4] P.J. Waller, F. Gandara, O.M. Yaghi, Acc. Chem. Res. 48 (2015) 3053.
[5] J. Jiang, Y. Zhao, O.M. Yaghi, J. Am. Chem. Soc. 138 (2016) 3255.
[6] F. Haase, B.V. Lotsch, Chem. Soc. Rev. 49 (2020) 8469.
[7] S. Kandambeth, K. Dey, R. Banerjee, J. Am. Chem. Soc. 141 (2019) 1807.
[8] J. Hu, S.K. Gupta, J. Ozdemir, M.H. Beyzavi, ACS Appl. Nano Mater. 3 (2020) 6239.
[9] N. Huang, P. Wang, D. Jiang, Nat. Rev. Mater. 1 (2016) 16068.
[10] Y. Guan, F. Chen, Q. Fang, S. Qiu, Chem. Soc. Rev. 49 (2020) 1357.
[11] L. Bourda, C. Krishnaraj, P. Voort, K.V.J.M.A. Hecke, Mater. Adv. 2 (2021) 2811.
[12] B. Gui, G. Lin, H. Ding, C. Gao, A. Mal, C. Wang, Acc. Chem. Res. 53 (2020) 2225.
[13] Z. Wang, S. Zhang, Y. Chen, Z. Zhang, S. Ma, Chem. Soc. Rev. 49 (2020) 708.
[14] J.L. Segura, M.J. Mancheno, F. Zamora, Chem. Soc. Rev. 45 (2016) 5635.
[15] J. Feng, J. Feng, X. Ji, C. Li, S. Han, H. Sun, M. Sun, TrAC Trends Anal. Chem. 137 (2021) 116208.
[16] N. Huang, L. Zhai, H. Xu, D. Jiang, J. Am. Chem. Soc. 139 (2017) 2428.
[17] A. Nagai, Z. Guo, X. Feng, S. Jin, X. Chen, X. Ding, D. Jiang, Nat. Commun. 2 (2011) 536.
[18] J.L. Segura, S. Royuela, M. Mar Ramos, Chem. Soc. Rev. 48 (2019) 3903.
[19] Y. Yusran, Q. Fang, S. Qiu, Isr. J. Chem. 58 (2018) 971.
[20] X. Liu, D. Huang, C. Lai, G. Zeng, L. Qin, H. Wang, H. Yi, B. Li, S. Liu, M. Zhang, R. Deng, Y. Fu, L. Li, W. Xue, S. Chen, Chem. Soc. Rev. 48 (2019) 5266.
[21] L. Zhu, Y.B. Zhang, Molecules 22 (2017) 1149.
[22] J. Zhang, J. Chen, S. Peng, S. Peng, Z. Zhang, Y. Tong, P.W. Miller, X.-P. Yan, Chem. Soc. Rev. 48 (2019) 2566.
[23] X. Kou, L. Tong, S. Huang, G. Chen, F. Zhu, G. Ouyang, TrAC Trends Anal. Chem. 136 (2021) 116182.
[24] H.J. Da, C.X. Yang, X.P. Yan, Environ. Sci. Technol. 53 (2019) 5212.
[25] S. Jansone-Popova, A. Moinel, J.A. Schott, S.M. Mahurin, I. Popovs, G.M. Veith, B.A. Moyer, Environ. Sci. Technol. 53 (2019) 878.
[26] J.M. Liu, X.Z. Wang, C.Y. Zhao, J.L. Hao, G.Z. Fang, S. Wang, J. Hazard Mater. 344 (2018) 220.
[27] W. Li, Y. Li, H.L. Qian, X. Zhao, C.X. Yang, X.P. Yan, Talanta 204 (2019) 224.
[28] S.L. Ji, H.L. Qian, C.X. Yang, X. Zhao, X.P. Yan, ACS Appl. Mater. Interfaces 11 (2019) 46219.
[29] Q. Sun, B. Aguila, J. Perman, L.D. Earl, C.W. Abney, Y. Cheng, H. Wei, N. Nguyen, L. Wojtas, S. Ma, J. Am. Chem. Soc. 139 (2017) 2786.
[30] S.Y. Ding, M. Dong, Y.W. Wang, Y.T. Chen, H.Z. Wang, C.Y. Su, W. Wang, J. Am. Chem. Soc. 138 (2016) 3031.
[31] H. Yuan, N. Li, J. Linghu, J. Dong, Y. Wang, A. Karmakar, J. Yuan, M. Li, P.J.S. Buenconsejo, G. Liu, H. Cai, S.J. Pennycook, N. Singh, D. Zhao, ACS Sens. 5 (2020) 1474.
[32] Y. Zhang, H. Li, J. Chang, X. Guan, L. Tang, Q. Fang, V. Valtchev, Y. Yan, S. Qiu, Small 17 (2021), e2006112.
[33] Z. Li, H. Li, X. Guan, J. Tang, Y. Yusran, Z. Li, M. Xue, Q. Fang, Y. Yan, V. Valtchev, S. Qiu, J. Am. Chem. Soc. 139 (2017) 17771.
[34] L. He, S. Liu, L. Chen, X. Dai, J. Li, M. Zhang, F. Ma, C. Zhang, Z. Yang, R. Zhou, Z. Chai, S. Wang, Chem. Sci. 10 (2019) 4293.
[35] W.-R. Cui, C.-R. Zhang, W. Jiang, F.-F. Li, R.-P. Liang, J. Liu, J.-D. Qiu, Nat. Commun. 11 (2020) 436.
[36] W.-R. Cui, C.-R. Zhang, R.-H. Xu, X.-R. Chen, W. Jiang, Y.-J. Li, R.-P. Liang, L. Zhang, J.-D. Qiu, Appl. Catal. B Environ. 294 (2021) 120250.
[37] H.L. Qian, C.X. Yang, X.P. Yan, Nat. Commun. 7 (2016) 12104.
[38] X. Wu, X. Han, Q. Xu, Y. Liu, C. Yuan, S. Yang, Y. Liu, J. Jiang, Y. Cui, J. Am. Chem. Soc. 141 (2019) 7081.
[39] X. Han, J. Huang, C. Yuan, Y. Liu, Y. Cui, J. Am. Chem. Soc. 140 (2018) 892.
[40] S. Zhang, Y. Zheng, H. An, B. Aguila, C.X. Yang, Y. Dong, W. Xie, P. Cheng, Z. Zhang, Y. Chen, S. Ma, Angew. Chem. Int. Ed. 57 (2018) 16754.

[41] J.-X. Guo, H.-L. Qian, X. Zhao, C. Yang, X.-P. Yan, J. Mater. Chem. A 7 (2019) 13249.
[42] Q. Gao, X. Li, G.-H. Ning, K. Leng, B. Tian, C. Liu, W. Tang, H.-S. Xu, K.P. Loh, Chem. Commun. 54 (2018) 2349.
[43] S. Dalapati, S. Jin, J. Gao, Y. Xu, A. Nagai, D. Jiang, J. Am. Chem. Soc. 135 (2013) 17310.
[44] J. Zhang, Z. Chen, S. Tang, X. Luo, J. Xi, Z. He, J. Yu, F. Wu, Anal. Chim. Acta 1089 (2019) 66.
[45] H.-J. Da, C.-X. Yang, H.-L. Qian, X.-P. Yan, J. Mater. Chem. A 8 (2020) 12657.
[46] H.L. Qian, F.L. Meng, C.X. Yang, X.P. Yan, Angew. Chem. Int. Ed. 59 (2020) 17607.
[47] C.X. Yang, C. Liu, Y.M. Cao, X.P. Yan, Chem. Commun. 51 (2015) 12254.
[48] T. Bao, P. Tang, D. Kong, Z. Mao, Z. Chen, J. Chromatogr. A 1445 (2016) 140.
[49] S. Dalapati, E. Jin, M. Addicoat, T. Heine, D. Jiang, J. Am. Chem. Soc. 138 (2016) 5797.
[50] Q. Lu, Y. Ma, H. Li, X. Guan, Y. Yusran, M. Xue, Q. Fang, Y. Yan, S. Qiu, V. Valtchev, Angew. Chem. Int. Ed. 57 (2018) 6042.
[51] H.L. Qian, C. Yang, X.P. Yan, Chem. Commun. 54 (2018) 11765.
[52] X. Liu, C. Yang, H.-L. Qian, X.-P. Yan, ACS Appl. Nano Mater. 4 (2021) 5437.
[53] J. Huang, X. Han, S. Yang, Y. Cao, C. Yuan, Y. Liu, J. Wang, Y. Cui, J. Am. Chem. Soc. 141 (2019) 8996.
[54] Y. Liu, X. Yan, H.-S. Lu, W.-D. Zhang, Y.-X. Shi, Z.-G. Gu, Sensor. Actuator. B Chem. 323 (2020) 128708.
[55] W.K. Li, P. Ren, Y.W. Zhou, J.T. Feng, Z.Q. Ma, J. Hazard Mater. 388 (2020) 121740.
[56] Z.J. Yin, S.Q. Xu, T.G. Zhan, Q.Y. Qi, Z.Q. Wu, X. Zhao, Chem. Commun. 53 (2017) 7266.
[57] S. Karak, K. Dey, A. Torris, A. Halder, S. Bera, F. Kanheerampockil, R. Banerjee, J. Am. Chem. Soc. 141 (2019) 7572.
[58] M.W. Zhu, S.Q. Xu, X.Z. Wang, Y. Chen, L. Dai, X. Zhao, Chem. Commun. 54 (2018) 2308.
[59] W.-R. Cui, F.-F. Li, R.-H. Xu, C.-R. Zhang, X.-R. Chen, R.-H. Yan, R.-P. Liang, J.-D. Qiu, Angew. Chem. Int. Ed. 59 (2020) 17684.
[60] L. Zang, M. He, Z. Wu, B. Chen, B. Hu, J. Chromatogr. A 1659 (2021) 462647.
[61] C. Song, Y. Shao, Z. Yue, Q. Hu, J. Zheng, H. Yuan, A. Yu, W. Zhang, S. Zhang, G. Ouyang, Anal. Chim. Acta 1176 (2021) 338772.
[62] L. Liu, W.-K. Meng, L. Li, G.-J. Xu, X. Wang, L.-Z. Chen, M.-L. Wang, J.-M. Lin, R.-S. Zhao, Chem. Eng. J. 369 (2019) 920.
[63] Y. Zhao, X. Liu, Y. Li, M. Xia, T. Xia, H. Sun, Z. Sui, X.-M. Hu, Q. Chen, Microporous Mesoporous Mater. 319 (2021) 111046.
[64] S. He, T. Zeng, S. Wang, H. Niu, Y. Cai, ACS Appl. Mater. Interfaces 9 (2017) 2959.
[65] Y. Li, C.X. Yang, X.P. Yan, Chem. Commun. 53 (2017) 2511.
[66] L.L. Wang, C.X. Yang, X.P. Yan, Chempluschem 82 (2017) 933.
[67] X. Niu, W. Lv, Y. Sun, H. Dai, H. Chen, X. Chen, Microchim. Acta 187 (2020) 233.
[68] L.H. Liu, C.X. Yang, X.P. Yan, J. Chromatogr. A 1479 (2017) 137.
[69] L. Zhao, W. Lv, X. Niu, C. Pan, H. Chen, X. Chen, J. Chromatogr. A 1615 (2020) 460722.
[70] L.-L. Wang, C.-X. Yang, X.-P. Yan, Sci. China Chem. 61 (2018) 1470.
[71] Z. Li, N. Huang, K.H. Lee, Y. Feng, S. Tao, Q. Jiang, Y. Nagao, S. Irle, D. Jiang, J. Am. Chem. Soc. 140 (2018) 12374.
[72] N. Zhang, B. Wei, T. Ma, Y. Tian, G. Wang, J. Mater. Sci. 56 (2021) 11789.
[73] D. Li, Y. Chen, Z. Liu, Chem. Soc. Rev. 44 (2015) 8097.
[74] R.G. Pearson, J. Chem. Educ. 45 (1968) 643.
[75] W. Xu, X. Sun, M. Huang, X. Pan, X. Huang, H. Zhuang, J. Environ. Manag. 269 (2020) 110758.
[76] Y. Xiao, C. Ma, Z. Jin, C. Wang, J. Wang, H. Wang, X. Mu, L. Song, Y. Hu, Separ. Purif. Technol. 259 (2021) 118119.
[77] L. Guo, S. Jia, C.S. Diercks, X. Yang, S.A. Alshmimri, O.M. Yaghi, Angew. Chem. Int. Ed. 59 (2020) 2023.
[78] H.P. Ma, B.L. Liu, B. Li, L.M. Zhang, Y.G. Li, H.Q. Tan, H. Zhu, J. Am. Chem. Soc. 138 (2016) 5897.
[79] H. Chen, H. Tu, C. Hu, Y. Liu, D. Dong, Y. Sun, Y. Dai, S. Wang, H. Qian, Z. Lin, L. Chen, J. Am. Chem. Soc. 140 (2018) 896.
[80] F. Li, X. Zhang, X. Zhao, Nucl. Eng. Des. 322 (2017) 159.
[81] C.R. Zhang, W.R. Cui, R.H. Xu, X.R. Chen, J.D. Qiu, CCS Chem. 3 (2020) 1.
[82] R.-R. Liang, X. Zhao, Org. Chem. Front. 5 (2018) 3341.
[83] N. Li, J. Du, D. Wu, J. Liu, N. Li, Z. Sun, G. Li, Y. Wu, TrAC Trends Anal. Chem. 108 (2018) 154.
[84] W.H. Ji, Y.S. Guo, X. Wang, X.F. Lu, D.S. Guo, J. Chromatogr. A 1595 (2019) 11.
[85] S. Huang, G. Chen, N. Ye, X. Kou, F. Zhu, J. Shen, G. Ouyang, Anal. Chim. Acta 1077 (2019) 67.
[86] M. Wu, C. Gang, L. Ping, W. Zhou, Q. Jia, J. Chromatogr. A 1456 (2016) 34.
[87] I. Vasconcelos, C. Fernandes, TrAC Trends Anal. Chem. (Reference Ed.) 89 (2017) 41.
[88] Y.-Y. Lu, X.-L. Wang, L.-L. Wang, W. Zhang, J. Wei, J.-M. Lin, R.-S. Zhao, J. Hazard Mater. 407 (2021) 124782.
[89] S.N. Ghamat, Z. Talebpour, A. Mehdi, TrAC Trends Anal. Chem. (Reference Ed.) 118 (2019) 556.
[90] Y. Li, W. Chen, G. Xing, D. Jiang, L. Chen, Chem. Soc. Rev. 49 (2020) 2852.
[91] P. Zhang, Y. He, S. Wang, D. Shi, Y. Xu, F. Yang, J. Wang, L. He, Molecules 25 (2020) 3134.
[92] W. Sun, Y. Liu, W. Zhou, Z. Li, Z. Chen, Talanta 230 (2021) 122330.
[93] R. Xue, H. Guo, T. Wang, L. Gong, Y. Wang, J. Ai, D. Huang, H. Chen, W. Yang, Anal. Methods 9 (2017) 3737.
[94] L. Pu, Acc. Chem. Res. 50 (2017) 1032.
[95] Z.A. De Los Santos, S. MacAvaney, K. Russell, C. Wolf, Angew. Chem. Int. Ed. 59 (2020) 2440.